

Analysis of the soft switching modes for energy loss measurement of high frequency closed-loop boost converter

Ajoya Kumar Pradhan¹, Sarita Samal², Prasanta Kumar Barik³, Smrutiranjana Nayak¹

¹Department of Electrical and Electronics Engineering, Gandhi Institute of Technology and Management (GITAM), Bhubaneswar, India

²School of Electrical Engineering, KIIT Deemed to be University, Bhubaneswar, India

³Department of Electrical and Mechanical Engineering, College of Agricultural Engineering and Technology (CAET), Bhubaneswar, India

Article Info

Article history:

Received Nov 11, 2023

Revised Jul 26, 2024

Accepted Aug 15, 2024

Keywords:

AC-DC converter

DC-DC converter

Soft switching

Zero-current switching

Zero-voltage switching

ABSTRACT

This manuscript explains the analysis of the soft switching technology to measure the energy loss of high-frequency closed loop boost converter with zero-current switching (ZCS) and zero-voltage switching (ZVS) techniques. To get these attributes, the use of soft power converters that utilize soft switching techniques is essential. This paper examines the ZCS/ZVS AC/DC converter design, used in high-power systems for renewable energy and battery charging. This converter architecture ensures semiconductor switches turn on and off at zero voltage and current. It smooths rectifier diodes, reducing switching and reverse recovery losses. It has better power quality, efficiency, and input power factor. Practical study has been done to verify the converter's theoretical analysis. Empirical research shows gentle switching enhances system efficiency. Energy losses are reduced by 26% while turning on and 20% when turning off compared to the ZVS and ZCS. The prototype converter is built to corroborate simulation results. Compared to ZVS and ZCS, switching losses are lower and efficiency decline is modest across the operating range. This shows that the simulation and experimental results are consistent.

This is an open access article under the [CC BY-SA](#) license.



Corresponding Author:

Prasanta Kumar Barik

Department of Electrical and Mechanical Engineering

College of Agricultural Engineering and Technology (CAET)

Bhubaneswar, Odisha, India

Email: pkbarik.mee@ouat.ac.in

1. INTRODUCTION

High-frequency isolated DC-DC power conversion has drawn special attention in recent years from the fields of solid-state transformers, renewable energy power conversion, and microgrid power distribution [1]-[4]. High frequency isolated DC-DC power conversion's modular architecture provides high power density and good reliability two essentials for these kinds of applications. DC-DC converters are now an essential component of the system due to the growing amount of renewable energy that is being integrated into the grid. Both consumer electronics and industrial applications frequently employ DC-DC converters [5]. Therefore, the efficiency of these converters is necessary. The main cause of the DC-DC converter efficiency decline is switching losses [6]. When the converter is used at a high switching frequency and low power

output, this becomes very important [7]. Numerous soft switching strategies, including as zero-voltage switching (ZVS), zero-current switching (ZCS), and zero-voltage zero-current switching (ZVZCS), have been developed [8] to address this issue. When operating in these modes, switching loss, also known as voltage-current crossover, is minimized by manipulating the voltage and current transients [9]. To lower the crossover at both the turn-on and turn-off instants, ZVZCS concurrently controls both voltage and current transients. As a result, switching losses are significantly reduced, leading to increased efficiency. Specifically, this results directly from reducing the crossover losses by simultaneously manipulating the voltage and current transients. Nevertheless, neither this problem nor this analysis of the ZVZCS from this perspective was covered fully in the previous works. One can eventually get a general judgment about whether the ZVZCS approach is better or worse than the ZVS and ZCS. Further comprehension of soft switching methods and how DC-DC converters use them will also be improved by this.

In order to attain resonance and allow the diodes to function in the zero current switching (ZCS) state, the converter outlined in [9] makes advantage of the coupled inductor's leaking inductance. In [10], soft-switching is achieved by incorporating the resonant working mode into a traditional active-clamp coupled inductor converter via a hybrid transformer. Roy and Kapat [11] suggest using active clamp circuits with a shared clamp capacitor to achieve zero voltage switching (ZVS) for the primary power switch. Recent research [12], [13] developed a revolutionary high step-up non-isolated DC-DC converter that uses a connected inductor and voltage multiplier techniques. Zero-voltage switching (ZVS) is possible when the active switches are turned on, and zero-current switching (ZCS) is possible when the diodes are turned off. The converter uses two active switches and runs in resonant mode. The concept outlined in [14] combines a traditional inductor-based buck cell with a charge pump mechanism to reduce switch voltage stress and achieve a high voltage gain. Nevertheless, converters utilizing quasi-parallel resonant DC-link, as described in [14]-[16], typically need intricate control systems and incur a substantial overall cost. The most recent study on these converters is to minimize the quantity of auxiliary switches in order to streamline the control circuit and save costs. In order to decrease the number of auxiliary switches, additional components like as diodes, linked inductors, and capacitors are employed [17], [18]. Occasionally, the ability to regulate the DC-link zero voltage is also compromised, leading to the abrupt switching of switches.

However, the presence of intricate control systems is a significant worry in these topologies, primarily due to the need to address present sharing difficulties. The diode bridge or multi-pulse converters, which are conventional power converters, have been widely used for many years because of their high efficiency, dependability, and the widespread availability of power electronic components [19]-[21]. Nevertheless, the primary problems that restrict the utilization of front-end converters are elevated input current harmonics, diminished power factor, substantial weight, substantial volume, and elevated maintenance expenses [22]-[25].

2. PROPOSED METHOD

2.1. Soft switching analysis

By modeling the working model ZVZCS converter depicted in Figure 1, the soft modes of operation are presented. Since the switch-off scenario may be duplicated by changing a few basic factors, just the turn-on moment is chosen for investigation. The parameters and components of the experimental setup are presented in Table 1. Section 5 provides a description of pulse width modulation (PWM) switching. It should be noted that a metal oxide semiconductor field effect transistor (MOSFET's) switching transients are normal. An insulated-gate bipolar transistor (IGBT) can be subjected to the same analysis. Because of the tail current in this scenario, there would be a greater energy loss at the turn-off.

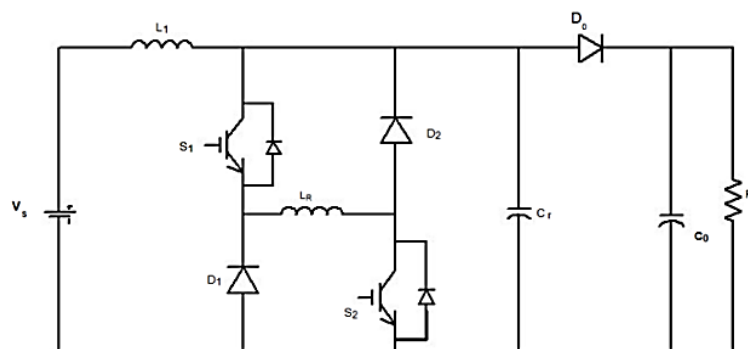


Figure 1. Soft switching boost converter

Table 1. Parameters and components of the experimental setup

Parameter	Value/Type
Input voltage	12 V
Output voltage	110 V
Switching frequency	20 kHz
Output filter capacitance	220 micro farads
Output filter inductance	1.5 mH
Rectifier diode	ON MBR 40250
Rectifier switch	IXFX 48N60P

2.2. Soft switching boost converter

Figure 1 illustrates the circuit schematic of a soft switching boost converter. A normal boost converter circuit is enhanced by using a soft switching cell, which comprises one inductor (L1), two capacitors (C1 and C2), and three diodes (D1, D2, and D3). An on/off control is accomplished with a single switch, and the switching loss may be minimized by switching at zero current and zero voltage, thanks to the resonances of the system.

2.2.1. Mode 1: operation of boost converter

The boost converter has six operating modes in a switching cycle, which are described in Figures 2-7. Both the switches S_1 and S_2 are in the off state. In this mode, the main inductor current decreases linearly and no current flows to the resonant inductor, and the resonant capacitor is charged as output voltage. The related mathematical models are also explained in (1)-(26).

$$V_L(t) = V_S - V_O \quad (1)$$

$$i_L(t) = i_L(t_0) - (V_O - V_S)t/L \quad (2)$$

$$i_{D0} = i_L(t) \quad (3)$$

2.2.2. Mode 2: operation of boost converter

Current flows to the resonant inductor as the switches S_1 and S_2 are ON. Here ZCS is achieved during the turn-on. As the resonant current rises linearly, the load current gradually decreases. When the resonant capacitor voltage equals to V_O , the output diode is cut off and then the mode 2 operation of the boost converter is completed.

$$i_{Lr}(i_1) = 0 \quad (4)$$

$$V_{Lr}(t) = V_O \quad (5)$$

$$i_{Lr}(t) = (V_O)t/Lr \quad (6)$$

$$i_L(t) = i_{Lr}(t_2) \quad (7)$$

$$i_{D0}(t_{20}) = 0 \quad (8)$$

2.2.3. Mode 3: operation of boost converter

The resonant capacitor C_r is released from V_0 to zero. In this configuration, the resonant inductor L_r and the capacitor C_r exhibit resonance, causing the voltage of C_r to decrease from the output voltage V_0 to zero. Here, the electric current from the primary inductor L passes through both the reluctance resistance (L_r) and the switch. A constant supply of power is provided to the load while the voltage at resonant mode C_{out} is being charged.

$$i_L(t_1) = I_{min} \quad (9)$$

$$V_{cr}(t_2) = V_O \quad (10)$$

$$V_{cr}(t_3) = 0 \quad (11)$$

$$W_r = \frac{1}{\sqrt{L_r C_r}} \quad (12)$$

$$Z_r = \sqrt{L_r / C_r} \quad (13)$$

2.2.4. Mode 4: operation of boost converter

This interval begins when the voltage of the resonant capacitor is zero. In this interval, the freewheeling diodes of D_1 and D_2 are turned on. The resonant inductor current flows to the freewheeling diodes S_1 - L_r - D_2 and S_2 - L_r - D_1 along the freewheeling path.

$$i_{Lr}(t) = i_L(t) + i_{D1}(t) + i_{D2}(t_2) \quad (14)$$

$$i_{Lr}(t_3) = i_{Lr}(t_4) = i_{Lrmax} \quad (15)$$

$$V_L(t) = V_s \quad (16)$$

$$i_L(t) = I_{min} + V_s(t)/L \quad (17)$$

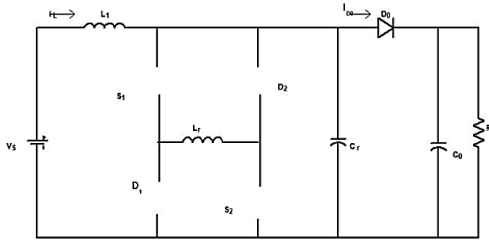


Figure 2. Mode 1 operation of boost converter

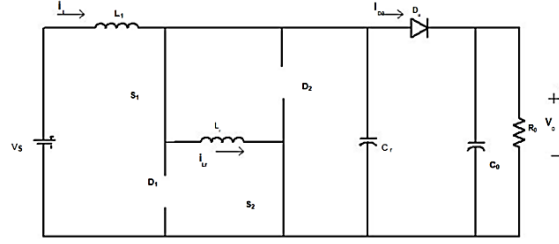


Figure 3. Mode 2 operation of boost converter

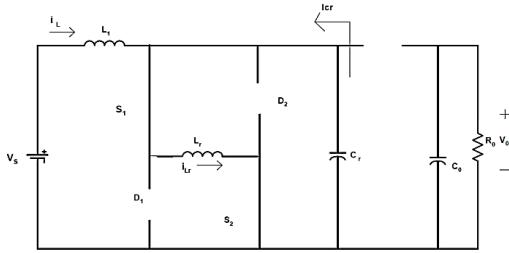


Figure 4. Mode 3 operation of boost converter

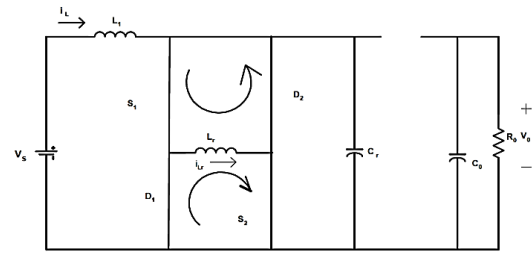


Figure 5. Mode 4 operation of boost converter

2.2.5. Mode 5: operation of boost converter

In this interval, switches are cut off under the zero-voltage condition by the resonant capacitor. During this interval, the inductor and capacitor voltages are presented in (18) to (21). Currently, there exist two operating current loops. The L_r - C_r - V_{in} loop is characterized by a linear expansion of the voltage of capacitor C_r from zero to the output voltage V_0 . Another loop is the L_r - C_r - D_1 loop, in which the second resonance has place.

$$i_{Lr}(t_4) = i_{Lrmax} \quad (18)$$

$$V_{Cr}(t_4) = 0 \quad (19)$$

$$i_L(t) = i_{Lrmax} \quad (20)$$

$$V_{Cr}(t_5) = V_0 \quad (21)$$

2.2.6. Mode 6: operation of boost converter

In this interval the output diode is turned on under zero voltage condition since the voltage across the resonant capacitor equals the output voltage. At this point, two of the inductor currents gradually diminish, and the energy stored in the resonant inductor is fully transferred to the load.

$$i_{D0}(t) = i_L(t) + i_{Lr}(t) \quad (22)$$

$$V_{cr}(t) = V_0 \quad (23)$$

$$i_L(t) = i_{max}(t) - (V_0 - V_s/L_r)t \quad (24)$$

$$i_{Lr}(t) = i_{Lr}(t_6) - (V_0/L_r)t \quad (25)$$

$$i_{Lr}(t_6) = 0 \quad (26)$$

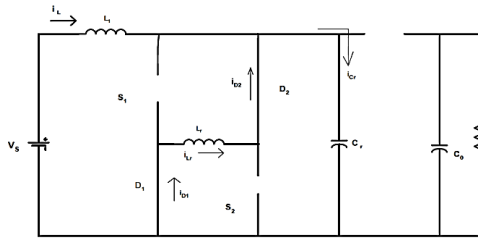


Figure 6. Mode 5 operation of boost converter

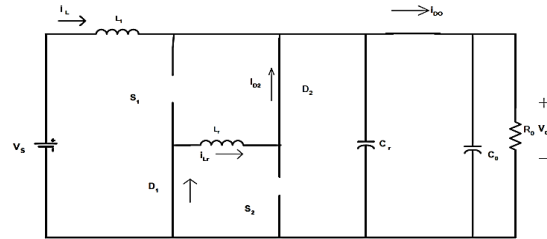


Figure 7. Mode 6 operation of boost converter

3. DETERMINATION OF CIRCUIT PARAMETERS AND UTILIZATION

3.1. Selection of V_s , R_0 , L_r , C_r , and V_o

The load resistance R_0 is selected according to the output power (27).

$$P = V_o^2/R_0 \quad (27)$$

Where P is power. Reducing the circuit volume is one benefit of high-frequency switching in power electronics. In actual use, inductance needs to be as little as feasible. If the capacitance's physical volume is not a concern, large capacitance is desired. The input voltage must not exceed the output voltage. For the controller design, the operating reference voltage V_o must be higher than the input voltage V_s .

3.2. Validation of the simulated circuit

Using the Simulink toolbox, a closed-loop simulation circuit for the boost converter is built, as seen in Figure 7. While designing the controller, the non-ideal circuit variables are considered but not taken into consideration. The inductor L 's series resistance and capacitor C are chosen. A resistor is utilized to produce step changes in the load resistance and a voltage source (V_s) is used to create step changes in the input voltage using perfect switches. The MOSFET switch and freewheeling diode's internal resistances and forward voltage dips are taken into account. They are simulated using parameters from off-the-shelf devices. Consideration is given to the settings for the freewheeling diodes $D1$ and $D2$. The MOSFET switch's current rating ensures that it will remain safe even during prolonged continuous current flow.

4. RESULTS AND DISCUSSION

The system's performance is contingent upon the following parameter values: step changes in the input voltage, resistance, inductance, and capacitance; step changes in the load resistance; disturbances in the input voltage; step changes in the reference voltage; and current ripple with realistic circuit parameters. Sensitivity analysis is performed under these conditions. The reference voltage is constant in the first four situations. Testing the controller's capacity to follow a reference voltage with step changes is the fifth case. The goal of the sixth instance is to show that the suggested controller can provide a usable current ripple with usable circuit specifications and a significantly lower maximum switching frequency. Comparing the system performances of ideal and practical circuits is the final scenario. Only the overall traveling direction of an output voltage transient (undershoot, overshoot, or no minimum phase) is examined in order to adjust the presentation loudness. A transient's rising time, overshoot amplitude, and settling time are not specifically examined. The analytical methods are also applicable to transients of inductor current; however, a thorough investigation is outside the purview of this thesis. Should the frequency of switching be lower than 10 kHz, the suggested controller will not operate. The bigger switching boundary layer is to blame for this. A system operating on these boundary layers diverges because it is essentially controlled by an open loop. The switching boundary layer shrinks as the switching frequency rises, improving the accuracy of the analysis and prediction. Based on an investigation with a maximum switching frequency of at least 20 kHz, the simulation findings are accurately represented. For every simulation, the beginning conditions $i(0) = 0$ and $v(0) = 0$ are applied.

4.1. System simulation

Figure 8 simulation model of closed loop boost converter simulation of closed-loop controlled boost converter is done using MATLAB and the results are presented for an input voltage of 200 V and an output voltage of 400 V and a switching frequency of 10 kHz. Figure 9 shows the switching pulse, voltage across the switch, and current through the switch. Figure 10 shows the current through the main inductor. Figure 11 shows the voltage across and current through the diode. Figure 12 shows the load voltage of the close loop boost converter with PI controller which is 400 V, two times greater than the input voltage.

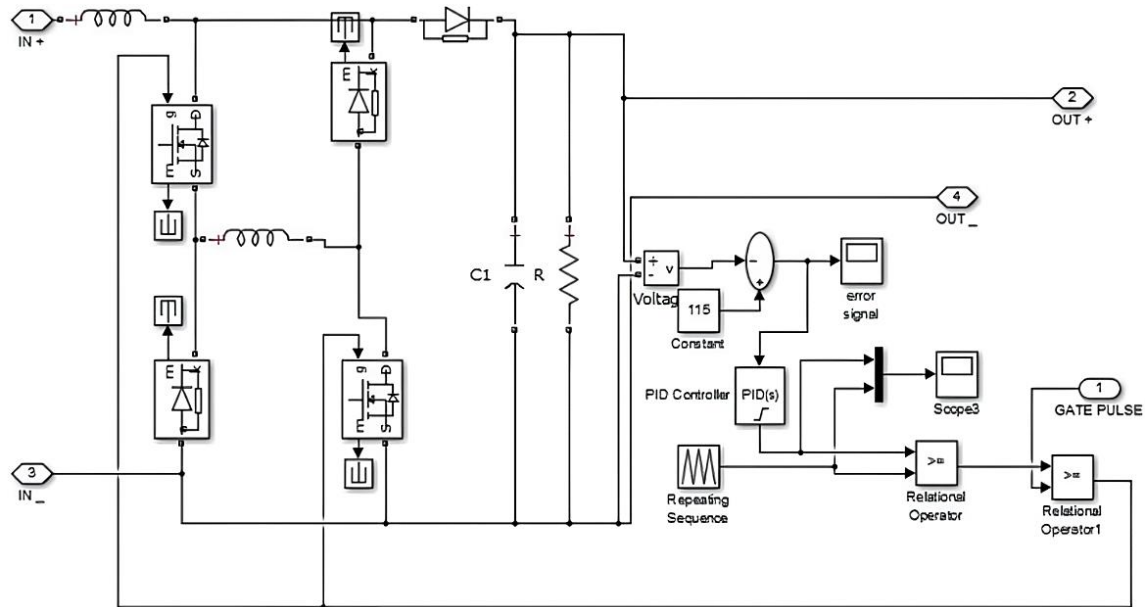


Figure 8. Closed loop simulation of boost converter

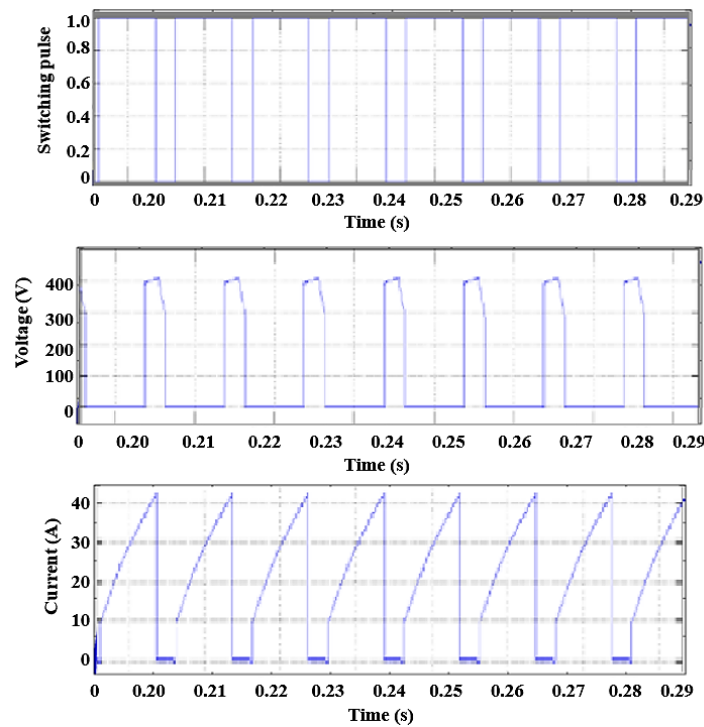


Figure 9. Simulation result of the switching pulse, voltage across the switch, and current through the switch

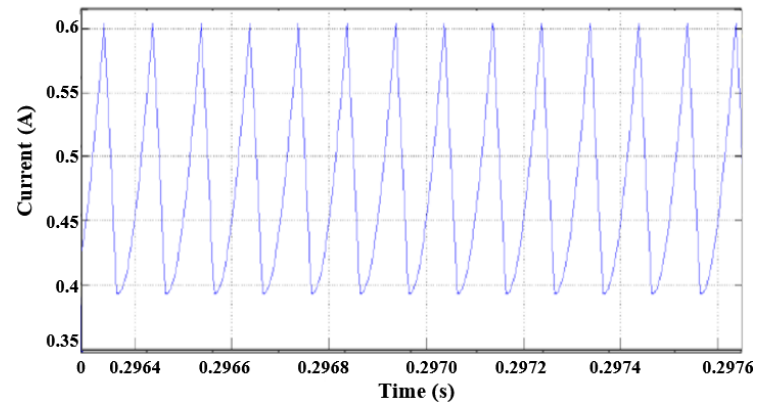


Figure 10. Simulated waveform of main inductor current in closed-loop

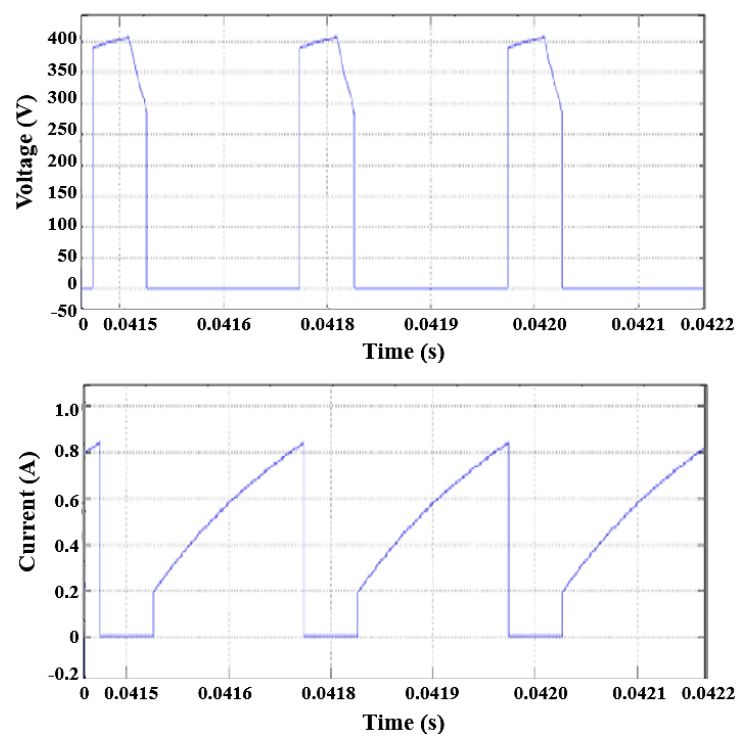


Figure 11. Simulated wave form of diode voltage and current in closed-loop

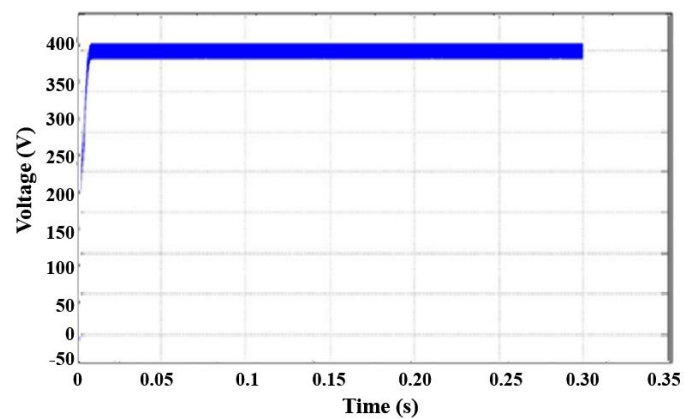


Figure 12. Simulated waveform of output voltage in closed-loop

4.2. Experimental setup for boost converter

A repeated waveform (sawtooth waveform) is compared with a signal level control voltage to provide the signal that governs the ON/OFF state of the switch. The saw tooth waveform frequency determines the switching frequency, while the voltage control level determines the duty ratio. The variation in the output voltage is crucial. A low-pass filter made of an inductor and a capacitor can be used to reduce this volatility.

The experimental setup of the boost converter is presented in Figure 13. The waveform of the experimental setup achieves the steady state value after 6 seconds. The steady-state value of the output voltage is 110 V. The suggested model's hardware is depicted in Figure 14. The output voltage of the experiment is shown in Figure 15. The overshoot becomes zero after 7 seconds. The output voltage, the voltage across diode D1, and the current through D1 are shown in Figure 16.

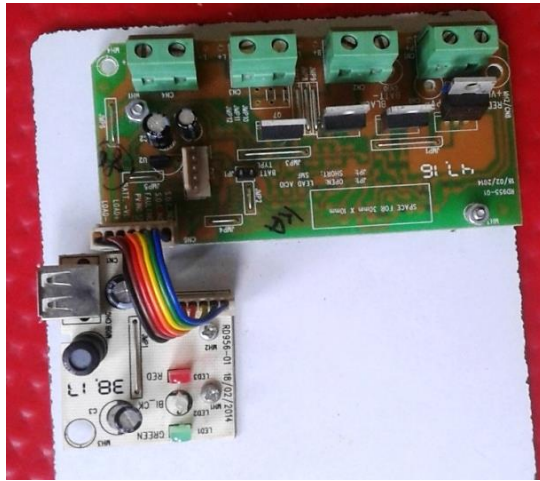


Figure 13. Hardware presentation of boost converter

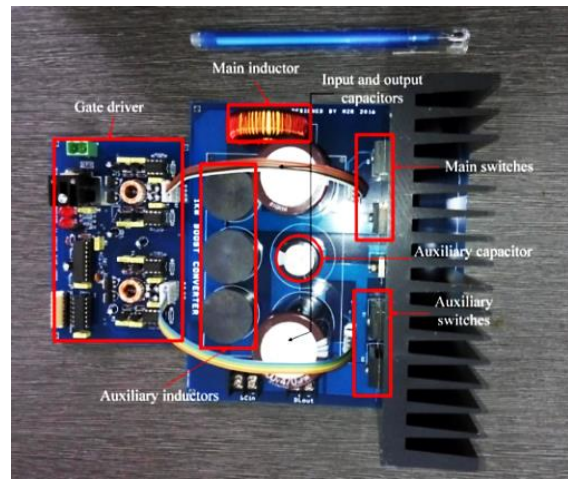


Figure 14. Hardware presentation of proposed model

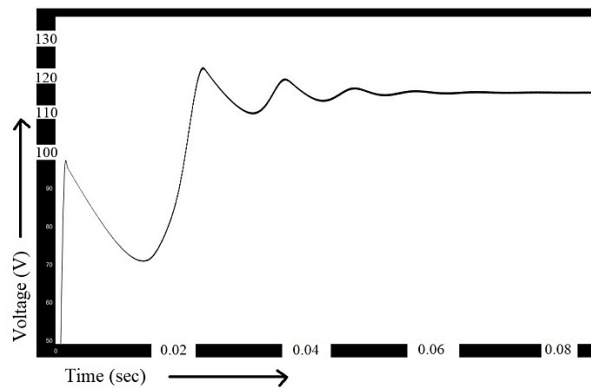


Figure 15. Simulated waveform of output voltage from experimental set up

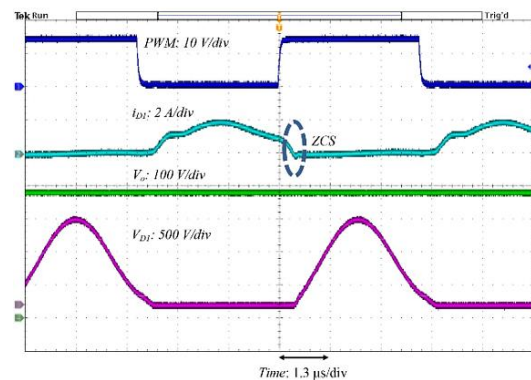


Figure 16. Experimental waveform of different voltage

5. CONCLUSION




This research examined the ZVZCS soft switching method. The advantages of the ZVZCS over the ZVS and ZCS in lowering switching losses and enhancing the soft switching range of operation was illustrated theoretically. It was discovered that the main reason for the improvement was that the ZVZCS was not significantly impacted by the variables that control the ZVS turn on and the ZCS turn off. A simulation test was conducted on many soft switching converters from the current literature in order to substantiate the theoretical assertion. Next, the major switches' turn-on and turn-off losses were measured. When compared to the ZVS and ZCS equivalents, respectively, the generated losses for the ZVZCS operation were found to be 26% and 20% lower, respectively. Moreover, the ZVZCS operation's modest standard deviation indicated

little departure from the typical loss profile throughout all operating phases. Future research can confirm ZVZCS's superior operability and efficiency compared to other comparable methods for a variety of converter types. In addition, it was found that, in contrast to the variations in switching frequency and input voltage, the efficiency decline was consistently maintained at a moderate and stable level.




REFERENCES

- [1] H. Fan and H. Li, "High-frequency transformer isolated bidirectional DC-DC converter modules with high efficiency over wide load range for 20 kVA solid-state transformer," *IEEE Transactions on Power Electronics*, vol. 26, no. 12, pp. 3599–3608, 2011, doi: 10.1109/TPEL.2011.2160652.
- [2] S. Inoue and H. Akagi, "A bidirectional isolated DC-DC converter as a core circuit of the next-generation medium-voltage power conversion system," *IEEE Transactions on Power Electronics*, vol. 22, no. 2, pp. 535–542, 2007, doi: 10.1109/TPEL.2006.889939.
- [3] B. Zhao, Q. Yu, and W. Sun, "Extended-phase-shift control of isolated bidirectional DC-DC converter for power distribution in microgrid," *IEEE Transactions on Power Electronics*, vol. 27, no. 11, pp. 4667–4680, 2012, doi: 10.1109/TPEL.2011.2180928.
- [4] G. Ortiz, J. Biela, D. Bortis, and J. W. Kolar, "1 megawatt, 20 kHz, isolated, bidirectional 12 kV to 1.2 kV DC-DC converter for renewable energy applications," in *2010 International Power Electronics Conference - ECCE Asia -, IPEC 2010*, 2010, pp. 3212–3219, doi: 10.1109/IPEC.2010.5542018.
- [5] R. H. Ashique and Z. Salam, "A family of true zero voltage zero current switching (ZVZCS) non-isolated bidirectional DC-DC converter with wide soft switching range," *IEEE Transactions on Industrial Electronics*, vol. 64, no. 7, pp. 5416–5427, 2017, doi: 10.1109/TIE.2017.2669884.
- [6] K. Mohammad, A. Ahad, M. S. Bin Arif, and R. H. Ashique, "Critical analysis and performance evaluation of solar PV-system implementing non-isolated DC-DC converters," in *2021 3rd International Conference on Sustainable Technologies for Industry 4.0, STI 2021*, 2021, pp. 1–6, doi: 10.1109/STI53101.2021.9732600.
- [7] X. Cui, C. Deng, and A. T. Avestruz, "A fast response DC-DC converter with programmable ripple for combined distributed computation and communication," in *Conference Proceedings - IEEE Applied Power Electronics Conference and Exposition - APEC*, 2021, pp. 468–473, doi: 10.1109/APEC42165.2021.9487391.
- [8] C. Bao, S. Guptam, and S. K. Mazumder, "Modeling and analysis of peak-current-controlled differential mode Ćuk inverter," in *Proceedings of the 2021 IEEE 12th International Symposium on Power Electronics for Distributed Generation Systems, PEDG 2021*, 2021, pp. 1–7, doi: 10.1109/PEDG51384.2021.9494167.
- [9] Y. Wang *et al.*, "Elimination of the interaction of the converters in switch-linear hybrid envelope tracking power supplies," *IEEE Transactions on Power Electronics*, vol. 35, no. 2, pp. 2053–2066, 2020, doi: 10.1109/TPEL.2019.2920148.
- [10] F. Chang, X. Cui, M. Wang, W. Su, and A. Q. Huang, "Large-signal stability criteria in DC power grids with distributed-controlled converters and constant power loads," *IEEE Transactions on Smart Grid*, vol. 11, no. 6, pp. 5273–5287, 2020, doi: 10.1109/TSG.2020.2998041.
- [11] R. Roy and S. Kapat, "Discrete-time framework for analysis and design of digitally current-mode-controlled intermediate bus architectures for fast transient and stability," *IEEE Journal of Emerging and Selected Topics in Power Electronics*, vol. 8, no. 4, pp. 3237–3249, 2020, doi: 10.1109/JESTPE.2020.2971513.
- [12] A. Ramyar, X. Cui, and A. T. Avestruz, "Two-port up/down DC-DC converter for two-dimensional maximum power point tracking of differential diffusion charge redistribution solar panel," in *2019 IEEE 20th Workshop on Control and Modeling for Power Electronics, COMPEL 2019*, 2019, pp. 1–8, doi: 10.1109/COMPEL.2019.8769644.
- [13] M. K. Al-Smadi and Y. Mahmoud, "Photovoltaic module cascaded converters for distributed maximum power point tracking: a review," *IET Renewable Power Generation*, vol. 14, no. 14, pp. 2551–2562, 2020, doi: 10.1049/iet-rpg.2020.0582.
- [14] M. Chiampi and L. Zilberti, "Induction of electric field in human bodies moving near MRI: An efficient BEM computational procedure," *IEEE Transactions on Biomedical Engineering*, vol. 58, no. 10 PART 1, pp. 2787–2793, 2011, doi: 10.1109/TBME.2011.2158315.
- [15] M. Mohammadi, E. Adib, and M. R. Yazdani, "Family of soft-switching single-switch PWM converters with lossless passive snubber," *IEEE Transactions on Industrial Electronics*, vol. 62, no. 6, pp. 3473–3481, 2015, doi: 10.1109/TIE.2014.2371436.
- [16] M. R. Mohammadi and H. Farzanehfard, "A new family of zero-voltage-transition nonisolated bidirectional converters with simple auxiliary circuit," *IEEE Transactions on Industrial Electronics*, vol. 63, no. 3, pp. 1519–1527, 2016, doi: 10.1109/TIE.2015.2498907.
- [17] S. Dusmez, A. Khaligh, and A. Hasanzadeh, "A zero-voltage-transition bidirectional DC/DC converter," *IEEE Transactions on Industrial Electronics*, vol. 62, no. 5, pp. 3152–3162, 2015, doi: 10.1109/TIE.2015.2404825.
- [18] Y. Liang, F. Xie, Y. Liu, B. Zhang, and D. Qiu, "A Zero-Voltage Switching Three-Level Nonisolated Bidirectional DC/DC Converter with a Lossless Passive Component Auxiliary Circuit and Design-Oriented Analysis," *International Journal of Circuit Theory and Applications*, 2024, doi: 10.1002/cta.4269.
- [19] R. H. Ashique *et al.*, "A comparative performance analysis of zero voltage switching class E and selected enhanced class E inverters," *Electronics*, vol. 10, no. 18, 2021, doi: 10.3390/electronics10182226.
- [20] M. M. Samy, A. Shawky, and M. Orabi, "Comparative Analysis of Class-D, Class-E, and Class EF Inverter Topologies for Multi-Megahertz," in *2023 IEEE Conference on Power Electronics and Renewable Energy (CPERE)*, 2023, pp. 1–6, doi: 10.1109/CPERE56564.2023.10119623.
- [21] A. Karafil, "Thinned-out controlled IC MPPT algorithm for class E resonant inverter with PV system," *Ain Shams Engineering Journal*, vol. 14, no. 5, p.101992, 2023, doi: 10.1016/j.asej.2022.101992.
- [22] M. Ahmadi, M. R. Mohammadi, E. Adib, and H. Farzanehfard, "Family of non-isolated zero current transition bi-directional converters with one auxiliary switch," *IET Power Electronics*, vol. 5, no. 2, pp. 158–165, 2012, doi: 10.1049/iet-pel.2011.0098.
- [23] Y. Ye, K. W. E. Cheng, and S. Chen, "A high step-up PWM DC-DC converter with coupled-inductor and resonant switched-capacitor," *IEEE Transactions on Power Electronics*, vol. 32, no. 10, pp. 7739–7749, 2017, doi: 10.1109/TPEL.2016.2633381.
- [24] B. Gu, J. Dominic, B. Chen, L. Zhang, and J. S. Lai, "Hybrid transformer ZVS/ZCS DC-DC converter with optimized magnetics and improved power devices utilization for photovoltaic module applications," *IEEE Transactions on Power Electronics*, vol. 30, no. 4, pp. 2127–2136, 2015, doi: 10.1109/TPEL.2014.2328337.
- [25] E. A. O. Barbosa, M. L. d. S. Martins, L. R. Limongi, R. C. Neto, and E. J. Barbosa, "A Current-Fed Transformer-Based High-Gain DC-DC Converter with Inverse Gain Characteristic for Renewable Energy Applications," *IEEE Transactions on Industrial Electronics*, vol. 71, no. 9, pp. 10864–10876, Sep. 2024, doi: 10.1109/TIE.2023.3340184.




BIOGRAPHIES OF AUTHORS

Dr. Ajoya Kumar Pradhan    received his B.Tech. in electrical and electronics engineering from Andhra University in 2005 and completed his M.Tech. in power electronics engineering at KIIT (Deemed to be University), Bhubaneswar in 2009. He earned his Ph.D. in electrical engineering from SOA University, Bhubaneswar in 2018. Presently, he serves as an associate professor in the Department of Electrical Engineering at GITAM, Bhubaneswar since 2008. His current research focuses on renewable energy sources and microgrids. He has authored over 20 research papers in international journals and conferences. He can be contacted at email: ajoya.p@gmail.com.






Dr. Sarita Samal    earned her B.Tech. (Hons) in electrical engineering from Berhampur University in 2003 and completed her M.Tech. in power system engineering at VSSUT, Burla in 2006. She obtained her Ph.D. in electrical engineering from VSSUT, Burla in 2019. Currently, she holds the position of Associate Professor-I in the Department of Electrical Engineering at KIIT Deemed to be University, Bhubaneswar. Her research interests encompass power quality, renewable energy sources, and microgrid technologies. She has authored over 50 research papers in international journals and conferences. Additionally, she has contributed 6 book chapters published by Elsevier, Taylor & Francis, and holds 5 patents. She can be contacted at email: ssamalfel@kiit.ac.in.



Dr. Prasanta Kumar Barik    received his B.Tech. in electrical engineering from Utkal University, India, and completed his M.Tech. in power electronics and drives from Kalinga Institute of Industrial Technology, India. He obtained his Ph.D. from Indian Institute of Technology (Indian School of Mines) in Dhanbad, India. His research interests revolve around power quality enhancement and the utilization of power electronics in non-conventional energy sources. He has authored over 35 research papers in international journals and conferences. Additionally, he has contributed 4 book chapters published by Elsevier and Taylor & Francis. He can be contacted at email: pkbarik.mee@ouat.ac.in.



Dr. Smrutiranjana Nayak    obtained his Ph.D. in electrical engineering from Siksha 'O' Anusandhan (Deemed to be University), Bhubaneswar in 2022. Presently, he holds the position of assistant professor in the Department of Electrical Engineering at IGIT, Sarang, India. With over 15 years of teaching and research expertise, he has authored or co-authored more than 19 papers in international refereed journals and international conferences. His research interests encompass renewable energy, distribution systems, artificial intelligence, power quality, and smart grid technologies. He can be contacted at email: smrutikiit40@gmail.com.